euspen's 22nd International Conference & Exhibition, Geneva, CH, May/June 2022
www.euspen.eu

A study of influence factors on form error and surface finish in the high-frequency ultrasonic vibration-assisted cutting of structured surfaces

Canbin Zhang[1], Chi Fai Cheung[1], Benjamin Bulla[2]

[1]*State Key Laboratory of Ultra-precision Machining Technology, Department of Industrial and Systems Engineering, The Hong Kong Polytechnic University, Hung Hom, Kowloon, Hong Kong, China*

[2]*son-x Gmbh, Aachen, Germany*

canbin.zhang@connect.polyu.hk

Abstract

Ultrasonic vibration-assisted cutting (UVAC) is able to improve material machinability. For an ultrasonic tooling system, vibration amplitude is a key factor to be controlled which has significant effect on tool trajectory, cutting ratio, lubrication condition, etc. It plays an important role in affecting the form error of the workpiece being machined. In this paper, the high-frequency ultrasonic vibration-assisted cutting (HFUVAC) system, UTS2 with a frequency of 104 kHz is used to study influence factors including vibration amplitude, slope angle of the target profile and workpiece material on form error and surface finish of the structured surface. The input current which is in proportion to vibration amplitude is set as 20, 30 and 40 mA with an amplitude of about 0.5 - 1.0 µm, to machine cosine structures with various maximum slope angles on easy-to-machine material (copper alloy) and hard-to-machine material (steel), respectively. An analytical and experimental investigation has been conducted. The results show that slope angle of the target profile and workpiece material have a larger effect on form error than vibration amplitude. In HFUVAC of hard-to-machine materials with a higher hardness, form error increases significantly with increasing slope angle of the target profile, due to less cut of material caused by indentation effect in the downhill profile.

Keywords: high-frequency, ultrasonic vibration-assisted cutting, vibration amplitude, form error, structured surface, ulra-precsion machining

1. Introduction

Ultrasonic vibration-assisted cutting (UVAC) improves material machinability, including chatter suppression [1], burr suppression [2], reduced tools wear [3] and better surface finish [4] due to lower cutting force and enhanced lubrication conditions [5]. Increasing ultrasonic frequency is effecitive to further improve the material machinability and reduce tool wear [6]. As a result, some scholars made use of the state-of-art and high-frequency ultrasonic tooling system (UTS2) to fabricate complex structures on steel [7] and high entropy alloy [8], achieving high-quality in terms of high form accuracy and good surface finish. However, little research has been found to study the influence factors including vibration amplitude, slope angle of target profile and workpiece material on form error and surface finish in the machining of three dimensional (3D) structured surfaces such as microlens array.

In UVAC of structure surfaces, tool tip is equipped with a high-frequency vibration, which leads to overcut of the target line, as shown in Fig. 1. Vibration amplitude and slope angle of the target line influence the amount of overcut. Moreover, instantaneous rake angle and clearance angle of the diamond tool changes considerably when the diamond tool moves upward and downward along the cutting direction to cut the 3D structured surfaces [9], which could change the cutting conditions and thereby influence the machining accuracy especially for hard-to-machine materials.

To study the effect of influence factors on the form error and surface finish of the structured surface, including vibration amplitude, slope angle of the target line and workpiece material, this paper aims to compare the machining form accuracy and surface finish of cosine 3D structures with various maximum slope angles, which are machined on copper alloy and steel workpiece by HFUVAC under different input current of UTS2.

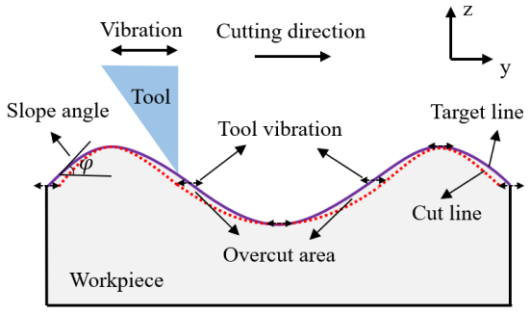

Figure 1. A schematic of overcut of material in UVAC.

2. Methods

2.1 Experimental parameters and setup

The tool path for the cosine 3D structure is defined by Eq. (1):

$$z(y) = \frac{h}{2}\cos\left(\frac{2\pi y}{\lambda}\right) - \frac{h}{2} \qquad (1)$$

where h and λ are the maximum depth and wavelength of the target line. Two cosine lines with the same maximum depth of 10 μm and various wavelengths of $\lambda_1 = 130\,um$ and $\lambda_2 = 390\,um$ were machined. These two profiles have a maximum slope angle of 13.8 ° and 4.6 °, respectively.

Fig. 2 shows the experimental setup to conduct the cutting experiments. An ultrasonic tooling system (UTS2 from Son-X GmbH Germany) with a working frequency of 104 kHz was configured on an ultraprecision machine (Moore Nanotech 350 FG from Nanotechnology Inc. USA).). A specific single crystal diamond insert with a tool nose radius of 1 mm, rake angle of 0 ° and clearance angle of 15 ° provided by Contour Fine tooling Ltd. was used. The workpiece materials are copper alloy and Mirrax 40. The input current of UTS2 was set at 20 mA, 30 mA and 40 mA with an amplitude of about 0.5 μm – 1.0 μm in the vertical direction, namely the cutting direction. To ensure successful fabrication of structured surfaces, cutting depth for the top position of structured surface was set as 1 μm. Cosine 3D structures were grooved by 4 tool paths with a cutting depth of 4 μm, 4 μm, 2 μm, and 1 μm, respectively, according to the programmed position code under a cutting speed of 100 mm/min. The position code was generated by Matlab software with a sampling rate of 2.5 μm along the cutting direction. The morphology and profile of the machined structure were measured by a Zygo white interferometer (Nexview, Zygo Ltd.).

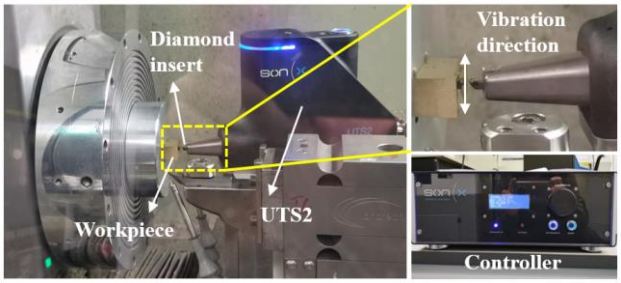

Figure 2. A photo of the experimental setup.

2.2 Theoretical form error induced by overcut in HFUVAC

The tool vibration is determined by Eq. (2):

$$y_1(t) = A\cos(2\pi f t) \tag{2}$$

where A is vibration amplitude f is vibration frequency. t is the cutting time. The tool movement driven by the machine slide is determined by Eq. (3):

$$\begin{cases} y_2(t) = v_c t \\ z_2(t) = \dfrac{h}{2}\cos\left(\dfrac{2\pi v_c t}{\lambda}\right) - \dfrac{h}{2} \end{cases} \tag{3}$$

where v_c represents the nominal cutting speed along the cutting direction. As a result, the tool track can be determined by Eq. (4):

$$\begin{cases} y(t) = y_1(t) + y_2(t) \\ z(t) = z_2(t) \end{cases} \tag{4}$$

The instant of front limit and back limit of tool track for each vibration cycle arise at the time when the tool velocity in the y-axis direction is zero. As a result, they can be determined by solving Eq. (5) as follows:

$$y(t)' = 0 \tag{5}$$

Based on these equations, the tool trajectory with the front-cut limit and back-cut limit in HFUVAC of the cosine line can be obtained. Fig. 3(a) shows the tool trajectory in HFUVAC of the cosine line with the wavelength of λ_1 under a vibration amplitude of 1 μm. In the downhill line, the back limit of tool track links up into a back-cut line left on the workpiece. While in the uphill line, the front limit of tool track constitutes a front-cut line left on the workpiece. As a result, there exists a deviation between the target profile and the cut profile, resulting in the theoretical form error as shown in Fig. 3(b). Fig. 4 presents the theoretical form error of the cosine profile with the wavelength of λ_1 and λ_2, under the vibration amplitude of 0.5 μm, 0.75 μm and 1.0 μm It is found that the largest form error appeared at the position with the maximum slope angle. Besides, form error increased with increasing vibration amplitude and the decreasing wavelength (or increasing maximum slope angle) of the cosine line.

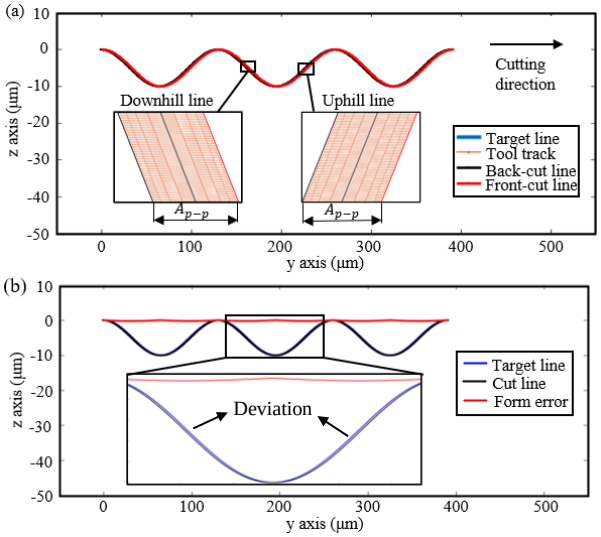

Figure 3. (a) Tool trajectory in UVAC of cosine line, (b) a comparison of the target line and cut line, with the wavelength of $\lambda_1$under a vibration amplitude of 1 um .

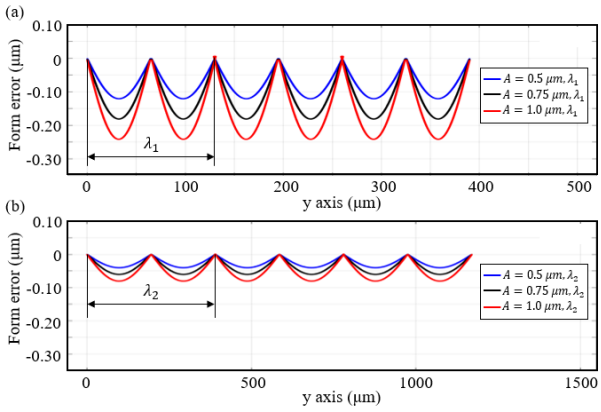

Figure 4. Theoretical form error of the cosine profile with various wavelength: (a) λ_1, (b) λ_2, under the vibration amplitude of 0.5, 0.75 and 1.0 um.

3. Results and discussions

3.1 HFUVAC of cosine structures on copper alloy workpiece

The form error of the machined cosine structure on copper alloy with three wavelengths was obtained after matching the two endpoints of the target profile and the cut profile as shown in Fig. 5. Fig. 6 shows the results of the form error for the machined cosine profile with the wavelength of λ_1 and λ_2, under the input current of 20 mA, 30 mA and 40 mA. The form error increased with decreasing the wavelength of cosine profile. For the structure with the wavelength of λ_2, the form error was small and comparable to the theoretical form error. However, for the structure with the wavelength of λ_1, it is interesting to note that the machined form error was much smaller and exhibited a different trend of variation as compared with the therectical form error. The effect of input current on form error was insignificant. These reflected that the machined profile was

not consistent with the theoretical cut line left on the workpiece as simulated. As a result, it is concluded that the effect of vibration amplitude on the form error is not as large as theoretical calculation. Besides, the form error showed a sudden increase in the downhill line which could be caused by material recovery due to the indentation effect during the tool downward movement [10]. Nevertheless, the form error of the machined structures were still quite small, and the surface finish of the machined structures after removing the structure from achieved an optical opplication level with surface roughness Sa = 2-3 nm as presented in Fig. 7.

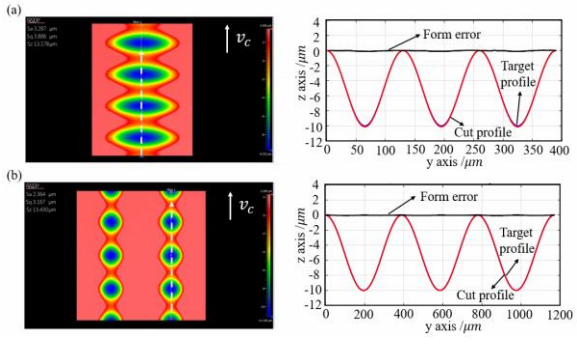

Figure 5. Measured structure morphology and comprison of the target profile (blue line) and cut profile (red line) for the cosine profiles with a wavelength of : (a) λ_1; (b) λ_2, under the input current of 20 mA. (worpiece material: copper alloy)

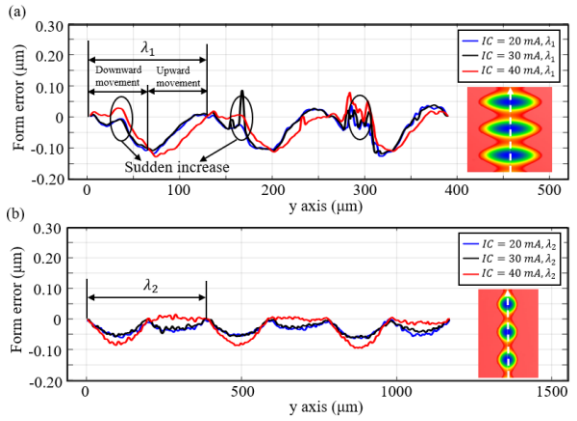

Figure 6. Form error of the machined cosine structure with various wavelength: (a) λ_1, (b) λ_2, under the input current of 20, 30 and 40 mA. (worpiece material: copper alloy)

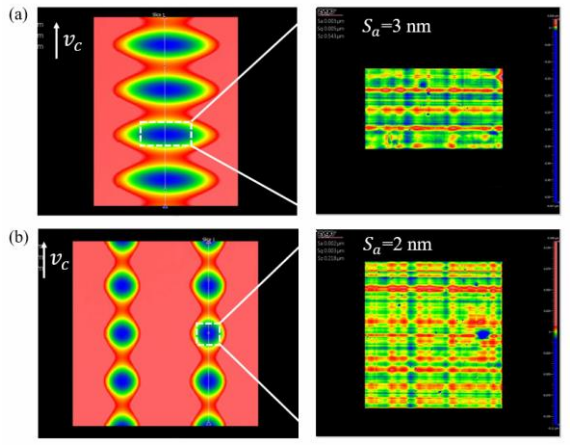

Figure 7. Measured structure morphology and surface roughness of the cosine profiles with a wavelength of : (a) λ_1; (b) λ_2, under the input current of 20 mA. (worpiece material: copper alloy)

3.2 HFUVAC of cosine structures on Mirrax 40 steel workpiece

Fig. 8 shows the matching result of the machined cosine structure with three wavelengths on Mirrax 40 steel, with a considerable form error for the structure with the wavelength of λ_1, or with a large maximum slope angle. Fig. 9 shows the result of form error for the machined cosine profile with the wavelength of λ_1 and λ_2, under the input current of 20, 30 and 40 mA. For the structure with the wavelength of λ_2, form error was still small and comparable to that of copper alloy. The form error increased significanly with decreasing wavelength, or increasing maximum slope angle. For the structure with the wavelength of λ_1, the effect of input current on form error was negligible. The machined form error with various input currents were too large (more than 0.4 μm) in consideration of the fact that a form error of less than 0.3 μm is acceptable for ultra-precision machining. The sudden increases in the downhill profile were much larger than those of copper alloy, suggesting that the indentation force was larger for hard-to-machine materials with higher hardness and for the structure with larger slope angle, leading to a larger amount of material recovery.

Fig. 10 shows the measured structure morphology and surface roughness after removing the structure form. As the from error is large for the structure with the wavelength of λ_1 and this caused difficulty in removing the structure form, the surface finish of the machined structure was divided into two parts according to tool downward and upward movement. The surface finish of the machined structures achieved an optical application level with a surface roughness s_a of 4-5 nm. The undulating texture in the downhill profile as presented in Fig. 10 (a) could support the existence of larger indentation force.

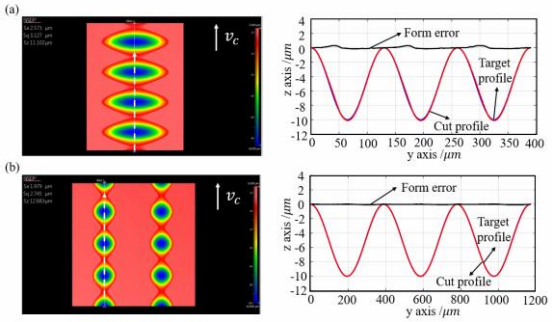

Figure 8. Measured structure morphology and comprison of the target profile (blue line) and cut profile (red line) for the cosine profiles with a wavelength of : (a) λ_1; (b) λ_2, under the input current of 20 mA. (worpiece material: Mirrax 40 steel)

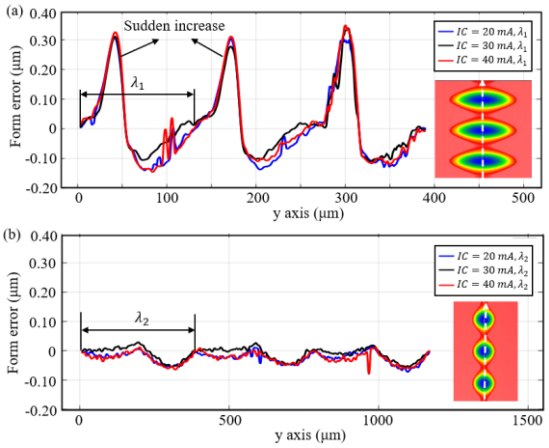

Figure 9. Form error of the machined cosine structure with various wavelength: (a) λ_1, (b) λ_2, under the input current of 20, 30 and 40 mA. (worpiece material: Mirrax 40 steel)

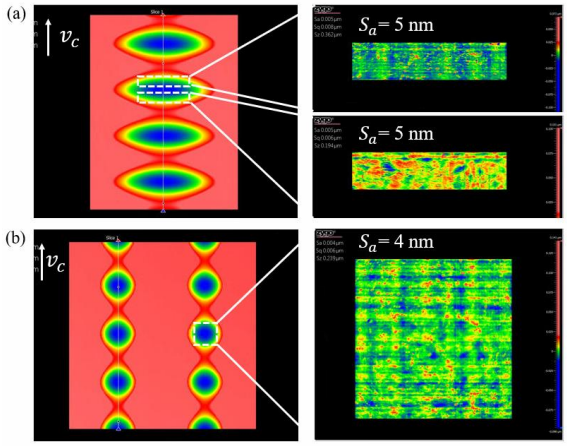

Figure 10. Measured structure morphology and surface roughness of the cosine profiles with a wavelength of : (a) λ_1; (b) λ_2, under the input current of 30 mA. (worpiece material: Mirrax 40 steel)

4. Conclusions

This study investigates the effect of vibration amplitude, slope angle of the target profile and workpiece material on the form error and surface finish of the structured surface being machined by HFUVAC. The surface morphology and form accuracy of cosine profiles machined on copper alloy and Mirrax 40 steel workpiece, with various maximun slope angles, under different input current of UTS2 were measured and analyzed. Some findings are given as follows:

The slope angle of the target profile and the workpiece material have a larger effect on form error than vibration amplitude. The vibration amplitude only has a noticeable but limited effect on the form error in HFUVAC of easy-to-machine material (copper alloy) with a relatively large maximum slope angle. By contrast, in HFUVAC of hard-to-machine material (Mirrax 40 steel), form error increases significantly with increasing slope angle of the target profile. The reduced cut of material is caused by material recovery possibly due to the indentation effect during the tool downward movement in the downhill profile. In the future, efforts will be made to reduce this effect, to further improve form accuracy of the structure surfaces with large slope angle and achieved a practical form error of less than 0.3 μm in HFUVAC of hard-to-machine materials. In view of the surface quality, all structures on copper alloy and Mirrax 40 steel machined by HFUVAC achieved an optical surface finish with nanometric surface roughness.

Acknowledgement

The authors would like to express their sincere thanks to the Innovation and Technology Commission (ITC) of the Government of the Hong Kong Special Administrative Region (HKSAR) for the financial support of the research work under the project (Projec code: GHP/142/19SZ) and the Research and Innovation Office (Project code: RK2Z) from The Hong Kong Polytechnic University. Special thanks are also due to the contract research project between the State Key Laboratory of Ultra-precision Machining Technology of The Hong Kong Polytechnic University and Son-X, Gmbh, Aachen, Germany.

References

[1] Xiao M, Sato K, Karube S and Soutome T 2003 The effect of tool nose radius in ultrasonic vibration cutting of hard metal. International *Int. J. Mach. Tools Manuf.* **43**(13) 1375–82

[2] Kim GD and Loh BG 2008 Characteristics of elliptical vibration cutting in micro-V grooving with variations in the elliptical cutting locus and excitation frequency *J. Micromech. Microeng.* **18**(2) 25002

[3] Suzuki N, Haritani M, Yang J, Hino R and Shamoto E 2007 Elliptical Vibration Cutting of Tungsten Alloy Molds for Optical Glass Parts *CIRP Ann-Manuf. Technol.* **56**(1) 127–30

[4] Zhang X, Senthil Kumar A, Rahman M, Nath C and Liu K 2011 Experimental study on ultrasonic elliptical vibration cutting of hardened steel using PCD tools *J. Mater. Process. Technol.* **211**(11) 1701–9

[5] Shamoto E and Moriwaki T 1999 Ultaprecision Diamond Cutting of Hardened Steel by Applying Elliptical Vibration Cutting *CIRP Ann-Manuf. Technol.* **48**(1) 441–4

[6] Klocke F, Dambon O, Bulla B and Heselhaus M 2008 Ultrasonic assisted turning of hardened steel with mono-crystalline diamond *In Proceedings of the 10th International Euspen Conference*

[7] Xing Y, Li C, Liu Y, Yang C and Xue C 2021 Fabrication of high-precision freeform surface on die steel by ultrasonic-assisted slow tool servo *Opt. Express* **29**(3) 3708–23

[8] Zhang L, Hashimoto T and Yan J 2021 Machinability exploration for high-entropy alloy FeCrCoMnNi by ultrasonic vibration-assisted diamond turning *CIRP Ann-Manuf. Technol.* **70**(1) 37–40

[9] Zhu W, Duan F, Zhang X, Zhu Z, and Ju B 2018 A new diamond machining approach for extendable fabrication of micro-freeform lens array *Int. J. Mach. Tools Manuf.* **124** 134–148

[10] Yuan W and Cheung CF 2021 Theoretical and experimental investigation of the tool indentation effect in ultra-precision tool-servo-based diamond cutting of optical microstructured surfaces *Opt. Express* **29** 39284–39303